

# Modeling Constrained Preemption Dynamics Of Transient Cloud Servers

Anonymous Author(s)

## ABSTRACT

Scientific computing applications are being increasingly deployed on cloud computing platforms. Transient servers can be used to lower the costs of running applications on the cloud. However, the frequent preemptions and resource heterogeneity of these transient servers introduces many challenges in their effective and efficient use. In this paper, we develop techniques for modeling and mitigating preemptions of transient servers, and present SciSpot, a software framework that enables low-cost scientific computing on the cloud. SciSpot deploys applications on Google Cloud preemptible virtual machines, and introduces the first empirical and analytical model for their preemptions.

SciSpot's design is guided by our observation that many scientific computing applications (such as simulations) are deployed as "bag" of jobs, which represent multiple instantiations of the same computation with different physical and computational parameters. For a bag of jobs, SciSpot finds the optimal transient server on-the-fly, by taking into account the price, performance, and preemption rates of different servers. SciSpot reduces costs by 5× compared to conventional cloud deployments, and reduces makespans by up to 10× compared to conventional high performance computing clusters.

## 1 INTRODUCTION

Transient cloud computing is an emerging and popular resource allocation model used by all major cloud providers, and allows unused capacity to be offered at low costs as preemptible virtual machines. Transient VMs can be unilaterally revoked and preempted by the cloud provider, and applications running inside them face fail-stop failures. Due to their volatile nature, transient VMs are offered at steeply discounted rates. Amazon EC2 spot instances [12], Google Cloud Preemptible VMs [7], and Azure Batch VMs [3], are all examples of transient VMs, and are offered at discounts ranging from 50 to 90% compared to conventional, non-preemptible "on-demand" VMs.

To expand the usability and appeal of transient VMs, many systems and techniques have been proposed that seek to ameliorate the effects of preemptions and reduce the computing costs of applications. Fault-tolerance mechanisms, resource management policies, and cost optimization techniques have been proposed for a wide range of applications—ranging from interactive web services, distributed data processing, parallel computing, etc. These techniques have been shown to minimize the performance-degradation and downtimes due to preemptions, and reduce computing costs by up to 90%.

However, the success of these techniques depends on probabilistic estimates of when and how frequently preemptions occur. For instance, many fault-tolerance and resource optimization policies are parametrized by the mean time to failure (MTTF) of the transient

VMs. For example, periodic checkpointing is a common technique for reducing the work lost due to preemptions, and the "optimal" checkpointing frequency that minimizes the total expected running time of a job depends on the MTTF of the VMs.

Past work on transient computing has focused on Amazon EC2's spot instances, whose preemption characteristics are determined by dynamic prices (which are in turn set using a continuous second-price auction). Transiency-mitigation techniques such as VM migration [62], checkpointing [51, 60], diversification [61], all use price-signals to model the availability and preemption rates of spot instances. However, these pricing-based models are not generalizable to other transient VMs having a flat price (such as Google's or Azure's offerings). In these cases, the lack of information about preemption characteristics precludes most failure modeling and transient computing optimizations.

To address this gap, we seek to understand the preemption characteristics of Google's Preemptible VMs, whose distinguishing characteristic is that they have a *maximum lifetime of 24 hours*. We conduct a large empirical study of over 1,500 preemptions of Google Preemptible VMs, and develop an analytical probability model of preemptions. We find that the temporal constraint is a radical departure from pricing-based preemptions, and presents fundamental challenges in preemption modeling and effective use of Preemptible VMs.

Due to the temporal preemption constraint, classical models that form the basis of preemption modeling and policies, such as memoryless exponential failure rates, are not applicable. We find that preemption rates are *not* uniform, but bathtub shaped with multiple distinct temporal phases, and are incapable of being modeled by existing bathtub distributions such as Weibull. We capture these characteristics by developing a new probability model. Our model uses reliability theory principles to capture the 24-hour lifetime of VMs, and generalizes to VMs of different resource capacities, geographical regions, and across different temporal domains. To the best of our knowledge, this is the *first* work on constrained preemption modeling. Our investigation also points to a new, surprising connection to statistical mechanics, which can lead to new insights for modeling temporally constrained events.

We show the applicability and effectiveness of our model by developing optimized policies for job scheduling, checkpointing, and server selection. These policies are fundamentally dependent on empirical and analytical insights from our model such as different time-dependent failure rates of different types of VMs. These optimized policies are a building block for transient computing systems and reducing the performance degradation and costs of preemptible VMs. We implement and evaluate these policies as part of a new software framework for running scientific computing applications, called Our service.

Our service abstracts typical scientific computing workloads and workflows into a new unit of execution, which we call as a "bag of jobs". These bags of jobs, ubiquitous in scientific computing,

117 represent multiple instantiations of the same application launched  
 118 with possibly different physical and computational parameters. The  
 119 bag of jobs abstraction permits efficient implementation of our  
 120 optimized policies, and allows Our service to lower the costs and  
 121 barriers of transient VMs for scientific computing applications.  
 122

Towards our goal of developing a better understanding of constrained preemptions, we make the following contributions:

- (1) We develop a probability model of constrained preemptions based on a large-scale, first-of-its-kind empirical study of lifetimes of Google Preemptible VMs for understanding and characterizing their preemption dynamics. Our model captures the key effects resulting from the 24 hour lifetime constraint associated with these VMs, and we analyze it through the lens of reliability theory and statistical mechanics.
- (2) We develop optimized policies for job scheduling, periodic checkpointing, and VM selection, that minimize the total time and cost of running applications. These policies are based on our preemption models, and reduce job running times by up to 40% compared to existing preemption models used for transient VMs.
- (3) We implement all our policies as part of a new framework, Our service, and evaluate the cost and performance of different representative scientific computing applications on the Google Cloud Platform. Compared to conventional cloud deployments, Our service can reduce costs of running bags of jobs by more than 5×, and when compared to dedicated HPC clusters, it can reduce the total turnaround time by up to an order of magnitude.

## 2 BACKGROUND

We now give an overview of transient cloud computing, and motivate the need for the bag of jobs abstraction in scientific computing workflows.

### 2.1 Transient Cloud Computing

Infrastructure as a service (IaaS) clouds such as Amazon EC2, Google Public Cloud, Microsoft Azure, etc., typically provide computational resources in the form of virtual machines (VMs), on which users can deploy their applications. Conventionally, these VMs are leased on an “on-demand” basis: cloud customers can start up a VM when needed, and the cloud platform provisions and runs these VMs until they are shut-down by the customer. Cloud workloads, and hence the utilization of cloud platforms, shows large temporal variation. To satisfy user demand, cloud capacity is typically provisioned for the *peak* load, and thus the average utilization tends to be low, of the order of 25% [23, 70].

To increase their overall utilization, large cloud operators have begun to offer their surplus resources as low-cost servers with *transient* availability, which can be preempted by the cloud operator at any time (after a small advance warning). These preemptible servers, such as Amazon Spot instances [2], Google Preemptible VMs [7], and Azure batch VMs [3], have become popular in recent years due to their discounted prices, which can be 7-10× lower than conventional non-preemptible servers. Due to their popularity among users, smaller cloud providers such as Packet [8] and Alibaba [1] have also started offering transient cloud servers.

However, effective use of transient servers is challenging for applications because of their uncertain availability [59, 62]. Preemptions are akin to fail-stop failures, and result in loss of the

application’s memory and disk state, leading to downtimes for interactive applications such as web services, and poor throughput for long-running batch-computing applications. Consequently, researchers have explored fault-tolerance techniques such as checkpointing [51, 60, 66] and resource management techniques [61] to ameliorate the effects of preemptions. The effect of preemptions is dependent on a combination of application resource and fault model, and mitigating preemptions for different applications remains an active research area [42].

### 2.2 Preemption Modeling of Transient VMs

Past work on transient computing has almost exclusively focused on the Amazon EC2 spot market, which has a radically different preemption model and dynamics compared to other transient cloud servers such as those offered by Google Cloud and Azure.

Launched in 2009, Amazon’s EC2 spot instances are the first example of transient cloud servers. The preemptions of EC2 spot instances are based on their *price*, which is dynamically adjusted based on the supply and demand of cloud resources. Spot prices are based on a continuous second-price auction, and if the spot price increases above a pre-specified maximum-price, then the server is preempted [17].

Thus, the time-series of these spot prices can be used for understanding preemption characteristics such as the frequency of preemptions and the “Mean Time To Failure” (MTTF) of the spot instances. Publicly available<sup>1</sup> historical spot prices have been used to characterize and model spot instance preemptions [62, 81]. For example, past work has analyzed spot prices and shown that the MTTFs of spot instances of different hardware configurations and geographical zones range from a few hours to a few days [57, 59, 74]. (Prateek: sigcomm paper)

However the price-based approach for inferring preemption characteristics is of limited utility. Other transient VMs such as those offered by Google and Azure have *flat* pricing, and price-based techniques for preemption modeling and cost optimization are not applicable. Furthermore, price-based techniques may be of limited value after Amazon’s recent change where preemptions were decoupled with pricing. To address this shortcomings, we develop *empirical* preemptions models for transient VMs. In particular, we focus on Google Preemptible VMs, whose preemption properties have been unknown so far. Additionally, their unique fixed lifetime leads to new challenges for conventional reliability theory models, and requires new modeling techniques, which we develop later in Section ??.

## 3 CONSTRAINED PREEMPTIONS OF GOOGLE PREEMPTIBLE VMs

To measure and improve the performance of applications running on transient cloud servers, it is critical to understand the nature and dynamics of their preemptions. In this section, we present empirical analysis of preemptions of Google Preemptible VMs, and develop new probabilistic models of their preemption rates.

175  
176  
177  
178  
179  
180  
181  
182  
183

184  
185  
186  
187  
188  
189  
190  
191  
192  
193  
194  
195  
196  
197  
198  
199  
200  
201  
202  
203  
204  
205

206  
207  
208  
209  
210  
211  
212  
213  
214  
215  
216  
217  
218

219  
220  
221  
222  
223  
224  
225  
226  
227  
228  
229  
230  
231

232

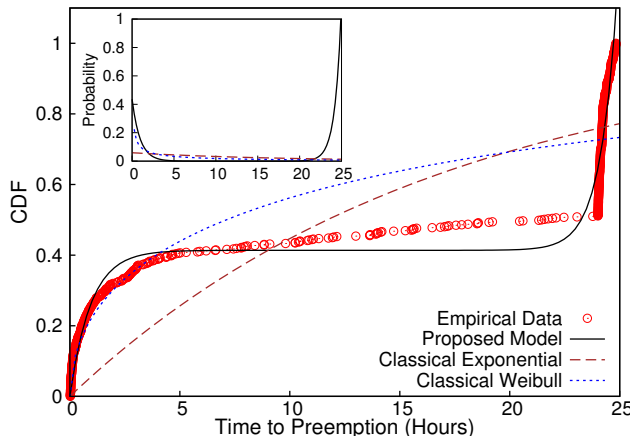


**Figure 1: CDF of lifetimes of Google Preemptible VMs. Our proposed distribution for modeling the constrained preemption dynamics provides better fits to the empirical data compared to the conventional exponential and the Weibull distributions. Inset shows the probability of failure as a function of time for the three distributions.**

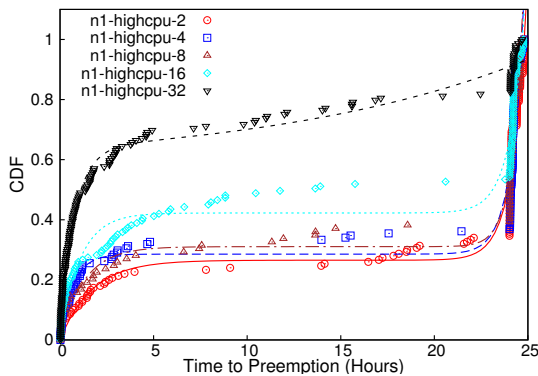


**Figure 2: Preemption characteristics of different VM types. Larger VMs are more likely to be preempted.**

### 3.1 Empirical Study Of Preemptions

To understand the nature of temporally constrained preemptions, we conducted the first empirical study of Google’s Preemptible VMs, that have a fixed price and a maximum 24 hour lifetime. Our empirical study is necessitated by the fact that the cloud operator (Google) does not disclose any other information about the preemption rates, and thus relatively little is known about the preemptions (and hence the performance) of these VMs.

We launched more than 1,500 Google Preemptible VMs of different types over a two month period (Feb–April 2019), and measured their time to preemption (i.e., their useful lifetime).<sup>2</sup>

A sample of over 100 such preemption events are shown in Figure 1, which shows cumulative distribution function (CDF) of the VM lifetimes of the n1-highcpu-16 VM in the us-east1-b

<sup>1</sup>Amazon posts Spot prices of 3 months, and researchers have been collecting these prices since 2010 [40].

<sup>2</sup>We will release the complete preemption dataset for further analysis.

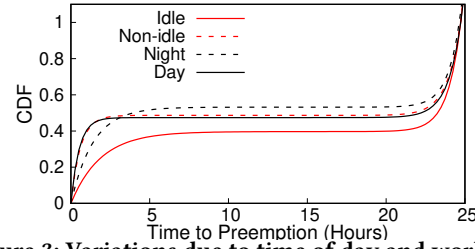


**Figure 3: Variations due to time of day and workload.**

zone. Note that the cloud operator (Google) caps the *maximum* lifetime of the VM to 24 hours, and all the VMs are preempted before that limit.

**Observation 1:** *The lifetimes of VMs are not uniformly distributed, but have three distinct phases.*

In the first (initial) phase, characterized by VM lifetime  $t \in [0, 3]$  hours, we observe that many VMs are quickly preempted after they are launched, and thus have a steep rate of failure (derivative of the CDF) initially. In the second phase, VMs that survive past 3 hours enjoy a relatively low preemption rate over a relatively broad range of lifetime (characterized by the slowly rising CDF in Figure 1). The third and final phase exhibits a steep increase in the number of preemptions as the preemption deadline of 24 hours approaches. The overall rate of preemptions is “bathtub” shaped as shown in the inset of Figure 1.

**Observation 2:** *The preemption behavior, imposed by the constraint of the small 24 hour lifetime, is substantially different from conventional failure characteristics of hardware components and even EC2 spot instances.*

In “classical” reliability analysis, the rate of failure usually follows an exponential distribution  $f(t) = \lambda e^{-\lambda t}$ , where  $\lambda = 1/\text{MTTF}$ . Figure 1 shows the CDF ( $= 1 - e^{-\lambda t}$ ) of the exponential distribution when fitted to the observed preemption data, by finding the distribution parameter  $\lambda$  that minimizes the least squares error. The classic exponential distribution is unable to model the observed preemption behavior because it assumes that the rate of preemptions is independent of the lifetime of the VMs, i.e., the preemptions are *memoryless*. This assumption breaks down when there is a fixed upper bound on the lifetime, as is the case for Google Preemptible VMs, and the conventional approach becomes insufficient to model this constrained preemption dynamics.

**Observation 3:** *The bathtub shaped preemption behavior is a general, universal characteristic of Preemptible VMs.*

In general, the preemption dynamics of a VM is determined by the supply and demand of VMs of that *particular* type. Thus, our empirical study looked at preemptions of VMs of different sizes, in different geographical zones, at different times of the day, and running different workloads (Figure YYY). In all cases, we find that the preemption behavior is bathtub shaped and has the three preemption phases. We argue that this is not a coincidence, but may be a result of practical and fundamental outcomes of cluster management policies.

While the actual specific preemption policy is up to the cloud operator, we will show that the bathtub behavior has benefits for applications. For applications that do not incorporate explicit fault-tolerance (such as checkpointing), early preemptions result in less wasted work than if the preemptions were uniformly distributed

349 over the 24 hour interval. Furthermore, the low rate of preemptions  
 350 in the middle periods allows jobs that are smaller than 24 hours to  
 351 finish execution with only a low probability of failure, once they  
 352 survive the initial preemption phase. We compare job performance  
 353 with bathtub shaped preemptions vs. uniform preemption rates in  
 354 Section Evaluation.

355 In addition to being beneficial to applications, we also conjecture  
 356 that the bathtub behavior is a *fundamental* characteristic of any  
 357 system where events are randomly distributed in a finite interval.  
 358 Intriguingly, we can analyze such temporally constrained preemptions  
 359 through a statistical mechanics framework, and we elaborate  
 360 on this connection later in Section ??.

361 **Observation 4:** *Larger VMs have a higher rate of preemptions.*

362 Figure 2 shows the preemption data from five different types of  
 363 VMs in the Google Cloud n1-highcpu-{2, 4, 8, 16, 32}, where the  
 364 number indicates the number of CPUs. All VMs are running in  
 365 the us-central1-c zone. We see that the larger VMs (16 and 32  
 366 CPUs) have a higher probability of preemptions compared to the  
 367 smaller VMs. While this could be simply due to higher demand for  
 368 larger VMs, it can also be explained from a cluster management  
 369 perspective. Larger VMs require more computational resources  
 370 (such as CPU and memory), and when the supply of resources  
 371 is low, the cloud operator can quickly reclaim a large amount of  
 372 resources by preempting larger VMs. This observed behavior aligns  
 373 with the guidelines for using preemptible VMs that suggests the  
 374 use of smaller VMs when possible [7].

375 **Observation 5:** *Preemptions exhibit diurnal variations, and are also  
 376 affected by the workload inside the VM.*

377 From Figure 3, we can see that VMs have a slightly longer lifetime  
 378 during the night (8 PM to 8 AM) than during the day. This is  
 379 expected because fundamentally, the preemption rates are higher  
 380 during periods of higher demand.

381 We also notice that completely idle VMs have longer lifetimes  
 382 than VMs running some workload. Presumably, this could be a  
 383 result of the lower resource utilization of idle VMs being more  
 384 amenable to resource overcommitment, and result in lower preemptions.

## 3.2 Failure Probability Model

388 We now develop an analytical probability model for preemption dynamics  
 389 that is faithful to the empirically observed data and provides  
 390 a basis for developing running-time and cost-minimizing optimizations.  
 391 Modeling temporally constrained preemptions raises many  
 392 challenges for existing preemption models that have been used for  
 393 other transient servers such as EC2 spot instances. We first discuss  
 394 why existing approaches to preemption modeling are not adequate,  
 395 and then present our closed-form probability model.

396 **3.2.1 Inadequacy of existing failure distributions.** Spot instance  
 397 preemptions have been modeled using exponential distribution [60?  
 398 ?], which is the default in most reliability theory applications.  
 399 However, the strict 24 hour constraint and the distinct preemption  
 400 phases are not compatible with the memoryless properties of the  
 401 exponential distribution. To describe failures (preemptions) that  
 402 are not memoryless (i.e., increasing or decreasing failure rate over  
 403 time), the classic Weibull distribution with CDF  $F(t) = 1 - e^{-(\lambda t)^k}$   
 404 is often employed. However, the Weibull distribution is also unable

407 to fit the empirical data (Figure 1) and especially unable to model  
 408 the sharp increase in preemptions near the 24 hour deadline.

409 For constrained preemptions, the increase in failure rate as modeled  
 410 by the Weibull distribution is not high enough. Other distributions,  
 411 such as Gompertz-Makeham, have also been used for modeling  
 412 bathtub behavior, especially for actuarial use-cases. The key  
 413 idea is to incorporate an exponential aging process, which is used  
 414 to model human mortality. The CDF of the Gompertz-Makeham  
 415 distribution is given by  $F(t) = 1 - \exp\left(-\lambda t - \frac{\alpha}{\beta}(e^{\beta t} - 1)\right)$  and is  
 416 fitted to the data in Figure XXX, and is also unable to provide a  
 417 good model for the observed preemption data.

418 The non-trivial bathtub-shaped failure rate of Google preemptible  
 419 VMs (Figure 1) requires models that capture the sudden onset of  
 420 the rise in preemptions near the deadline. From an application and  
 421 transiency policy perspective, the preemption model must provide  
 422 insights about the phase transitions, so that the application can  
 423 adapt to the sharp differences in preemption rates. For example,  
 424 the preemption model should be able to warn applications about  
 425 impending deadline, which existing failure distributions cannot  
 426 account for. Thus, not only is it important to minimize the total  
 427 distribution fitting error, it is also important to capture the changes  
 428 in phase. However, as we can see from the **QQ plots**, existing dis-  
 429 tributions are unable to capture the effects of the deadline and the  
 430 phases of the preemptions, and a new modeling approach is needed,  
 431 which we develop next.

432 **3.2.2 Multiple failure rate model.** Our failure probability model  
 433 seeks to address the drawbacks of existing reliability theory models  
 434 for modeling constrained preemptions. The key assumption under-  
 435 lying our model is the presence of two distinct failure processes.  
 436 The first process dominates over the initial temporal phase and  
 437 yields the classic exponential distribution that captures the high  
 438 rate of early preemptions. The second process dominates over the  
 439 final phase near the 24 hour maximum VM lifetime and is assumed  
 440 to be characterized by an exponential term that captures the sharp  
 441 rise in preemptions that results from this constrained lifetime.

442 Based on these observations, we propose the following general  
 443 form for the CDF:

$$\mathcal{F}(t) = A \left( 1 - e^{-\frac{t}{\tau_1}} + e^{\frac{t-b}{\tau_2}} \right) \quad (1)$$

444 where  $t$  is the time to preemption,  $1/\tau_1$  is the rate of preemptions in  
 445 the initial phase,  $1/\tau_2$  is the rate of preemptions in the final phase,  
 446  $b$  denotes the time that characterizes “activation” of the final phase  
 447 where preemptions occur at a very high rate, and  $A$  is a scaling  
 448 constant. In practice, typical fit values yield  $b \approx 24$  hours, and  
 449  $\tau_2 \approx 1$  hour, which ensures that our proposed distribution meets  
 450 the initial condition  $\mathcal{F}(0) \approx 0$ .

451 For most of its life, a VM sees failures according to the classic  
 452 exponential distribution with a rate of failure equal to  $1/\tau_1$  – this  
 453 behavior is captured by the  $1 - e^{-t/\tau_1}$  term in Equation 1. As VMs  
 454 get closer to their maximum lifetime imposed by the cloud operator,  
 455 they are reclaimed (i.e., preempted) at a high rate  $1/\tau_2$ , which is  
 456 captured by the second exponential term,  $e^{(t-b)/\tau_2}$  of Equation 1.  
 457 Shifting the argument ( $t$ ) of this term by  $b$  ensures that the expo-  
 458 nential reclamation is only applicable near the end of the VM’s  
 459 lifetime.

maximum lifetime and does not dominate over the entire temporal range.

The analytical model and the associated distribution function  $\mathcal{F}$  introduced above provides a much better fit to the empirical data (Figure 1) and captures the different phases of the preemption dynamics through parameters  $\tau_1$ ,  $\tau_2$ ,  $b$ , and  $A$ . These parameters can be obtained for a given empirical CDF using least squares function fitting methods. The failure or preemption rate can be derived from this CDF as:

$$f(t) = \frac{d\mathcal{F}(t)}{dt} = A \left( \frac{1}{\tau_1} e^{-t/\tau_1} + \frac{1}{\tau_2} e^{\frac{t-b}{\tau_2}} \right). \quad (2)$$

$p(t)$  vs.  $t$  yields a bathtub type failure rate function for the associated fit parameters (inset of Figure 1).

In the absence of any prior work on constrained preemption dynamics, our aim is to provide an interpretable model with a minimal number of parameters, that provides a sufficiently accurate characterization of observed preemptions data. Further generalization of this model to include more failure processes would introduce more parameters and reduce the generalization power. Exploring other approaches of modeling bathtub-type failure rates (e.g., exponential Weibull distributions) [24, 54] is part of our future work.

**3.2.3 Reliability Analysis.** We now analyze and place our model in a reliability theory framework.

**Expected Lifetime:** Our analytical model also helps crystallize the differences in VM preemption dynamics, by allowing us to easily calculate their expected lifetime. More formally, we define the expected lifetime of a VM of type  $i$ , as:

$$E[L_i] = \int_0^{24} t f_i(t) dt = -A(t + \tau_1)e^{-t/\tau_1} + A(t - \tau_2)e^{\frac{t-b}{\tau_2}} \Big|_0^{24} \quad (3)$$

where  $f_i(t)$  is the rate of preemptions of VMs of type  $i$  (Equation 2).

This expected lifetime can be used in lieu of MTTF, for policies and applications that require a “coarse-grained” comparison of the preemption rates of servers of different types, which is a key requirement in cost-minimizing server selection, which we develop later in Section.

**Hazard Rate:** We now compute the hazard rate of our model, which is defined as  $\lambda(t) = \frac{S(t)}{f(t)}$ , where  $S(t) = 1 - F(t)$  is the survival function. The hazard rate also related to the CDF as follows:  $1 - F(t) = \exp \int_0^t -\lambda(x) dx$ .

The hazard rate governs the dynamics of the failure processes. For example, the exponential distribution has a constant hazard rate  $\lambda$ . The Gompertz-Makeham distribution has an increasing failure rate to account for the increase in mortality, and its hazard rate is given by  $\lambda(t) = \lambda + \alpha e^{\beta t}$ . Since we model multiple failure rates and deadline-driven preemptions, our hazard rate also increases with time, and can be computed by simplifying

$$\lambda(t) = \frac{-r_1 e^{-r_1 t} - r_2 e^{r_2(t-b)}}{e^{-r_1 t} - e^{r_2(t-b)}}.$$

After algebraic simplification, we get a more interpretable hazard rate for our model:

$$\lambda = r_2 + \bar{r} \left( \frac{1}{1 - e^{-r_2 b} e^{\bar{r} t}} \right) = \frac{r_1 + r_2 e^{-r_2 b} e^{\bar{r} t}}{1 - e^{-r_2 b} e^{\bar{r} t}} \quad (4)$$

Here,  $\bar{r} = r_1 + r_2$ , ie., the sum of the two failure rate constants.

For ease of exposition, we can write this as:

$$\lambda = \frac{r_1 + \gamma_1 e^{\delta(t-b)}}{1 - \gamma_2 e^{\delta(t-b)}} \quad (5)$$

We note that the numerator is similar to the hazard rate of Gompertz-Makeham. The key difference is the  $1 - \gamma_2 e^{t-b}$  factor in the denominator. Recall that the sharp increase in preemption rate only happens close to the deadline, which means that  $b \leq 24$ . Thus, when  $t < b$ , we get a conventional  $\lambda = r_1$ , or the classic exponential distribution. As  $t$  approaches and exceeds  $b$ , the increase in failure rate kicks in, accounting for the deadline-driven rise in preemptions.

### 3.3 Connection to Statistical Mechanics

In addition to empirically-informed reliability models for preemptions, we also seek to understand *why* their distribution is bathtub shaped in order to provide a mechanistic understanding of preemptions and enhance the model interpretability and generalizability. To this end, we propose to “map” the problem of constrained preemptions to an equivalent problem of constrained many particle physical systems that can be analyzed employing the general theoretical framework of statistical mechanics.

A simple mapping can be established by assuming that the cluster management policy requires mutually exclusive preemptions. This assumption helps cluster management by serializing VM preemptions and making cluster operations easier, and it reduces the challenges associated with reacting to simultaneous preemptions. The preemption events become hard particles that cannot overlap. The probability distribution of  $N$  constrained preemption events gets mapped to the density of  $N$  randomly distributed particles confined in a 1-dimensional interval of length  $L$  (analogous to 24 hours). The particle size is equivalent to the length of the critical section, which is related to the preemption warning (30 seconds for Google PVMs). Finding the distribution of non-overlapping (i.e., hard) particles is a central problem in statistical mechanics [5]. This distribution is *not* uniform over the interval, but is higher towards the ends of the interval—analogous to the bath-tub shaped nature of preemptions!

The analytical framework suggests that the bath-tub shape of the probability distribution is the key characteristic of constrained preemptions. Therefore, our approach will remain relevant in the face of future changes in preemption characteristics due to changes in cloud usage and operational policies.

## 4 APPLICATION POLICIES FOR CONSTRAINED PREEMPTIONS

For applications running on transient servers, the effects of preemptions can be ameliorated through different policies for fault tolerance and resource management. Prior work in transient computing has established the benefits of such policies for a broad range of applications. We now show how our empirical insights and analytical model can be used to develop policies for optimized execution of batch applications on Google Preemptible VMs.

### 4.1 Job Scheduling

Many cloud-based applications and services are *long-running*, and typically run a continuous sequence of tasks and jobs on cloud servers. In the case of deadline-constrained bathtub preemptions,

581 applications face a choice: they can either run a new task on an  
 582 already running server, or relinquish the server and run the task on  
 583 a *new* server. This choice is important in the case of non-uniform  
 584 failure rates, since the job's failure probability depends on the "age"  
 585 of the server. Furthermore, since newly launched servers also have  
 586 high preemption rates (and thus high job failure probability), the  
 587 choice of running the job on an existing server vs. a new server is  
 588 not obvious.

589 Our job scheduling policy uses the preemption model to de-  
 590 termine the preemption probability of jobs of a given length  $T$ .  
 591 Assume that the running server's age (time since launch) is  $s$ . Then,  
 592 the the probability of failure on the existing server  $P_{\text{Existing}} = \max(1, F(T+s) - F(T))$ . The alternative is to discard the server  
 593 and launch a new server, in which case, the failure probability is  
 594  $P_{\text{New}} = F(T)$ . Depending on the server's age  $s$  and the job's run-  
 595 ning time  $T$ , we can compare  $P_{\text{Existing}}$  and  $P_{\text{New}}$ , and run the job  
 596 on whichever case yields the lower failure probability.  
 597

## 4.2 Periodic Checkpointing

600 A common technique for reducing the total expected running time  
 601 of jobs on transient servers is to use fault-tolerance techniques such  
 602 as periodic checkpointing [60]. Checkpointing application state to  
 603 stable storage (such as network file systems or centralized cloud  
 604 storage) reduces the amount of *wasted work* due to preemptions.  
 605 However, each checkpoint entails capturing, serializing, and writing  
 606 application state to a disk, and increases the total running time of  
 607 the application. Thus, the frequency of checkpointing can have a  
 608 significant effect on the total expected running time.  
 609

610 Existing checkpointing systems for handling hardware failures in  
 611 high performance computing, and for cloud transient servers such  
 612 as EC2 spot instances, incorporate the classic Young-Daly periodic  
 613 checkpointing interval that assumes that failures are exponentially  
 614 distributed. That is, the application is checkpointed every  $\tau = \sqrt{2 \cdot \delta \cdot \text{MTTF}}$  time units, where  $\delta$  is the time overhead of writing  
 615 a single checkpoint to disk.

616 However, checkpointing with a uniform period is sub-optimal in  
 617 case of time dependent failure rates, and especially for bathtub fail-  
 618 ure rates. A sub-optimal checkpointing rate can lead to increased  
 619 recomputation and wasted work, or result in excessive checkpoint-  
 620 ing overhead. Intuitively, the checkpointing rate should depend on  
 621 the failure rate, and our analytical preemption model can be used  
 622 for designing an optimized checkpointing schedule.

623 Let the uninterrupted running time of the job be  $T$ . Or in other  
 624 words,  $T$  amount of work needs to be performed. Let the checkpoint  
 625 cost be  $\delta$ . We seek to minimize the total expected running time  
 626 or the *makespan*, which is the sum of  $T$ , the expected periodic  
 627 checkpointing cost, and the expected recomputation.

628 The makespan  $M$  can be recursively defined and computed. Let  
 629  $M(W, t, i)$  denote the makespan when  $W$  length of job must be ex-  
 630 ecuted,  $t$  is amount of job already done. We now need to determine  
 631 when to take the *next* checkpoint, which we take after  $i$  steps. Let  
 632  $E[M^*]$  denote the minimum expected makespan.  
 633

$$E[M^*(W, t)] = \min_{0 < i \leq W} E[M(W, t, i)] \quad (6)$$

634 The makespan is affected by whether or not there is a failure  
 635 before we take the checkpoint:  
 636

$$E[M(W, t, i)] = P_{\text{succ}}(t, i + \delta) \cdot E[M_{\text{succ}}] + P_{\text{fail}}(i + \delta, t) \cdot E[M_{\text{fail}}] \quad (7)$$

637 Here  $P_{\text{succ}}(t, i + \delta)$  denotes the probability of the job successfully  
 638 executing without failures until the checkpoint is taken, i.e., from  $t$   
 639 to  $t + i + \delta$ .  $P_{\text{fail}}(i + \delta, t) = F(t + i + \delta) - F(i + \delta)$  is computed using  
 640 the CDF, and  $P_{\text{succ}} = 1 - P_{\text{fail}}$ .

641  $E[M_{\text{succ}}]$  is the expected makespan when there are no job failures  
 642 when the job is executing from step  $t$  to  $t + i + \delta$ , and is given by a  
 643 recursive definition:

$$E[M_{\text{succ}}(W, t, i)] = t + i + \delta + E[M^*(W - i, t + i + \delta)] \quad (8)$$

644 Note that the makespan includes the amount of work already done  
 645  $t + i$ , the checkpointing overhead  $\delta$ , and the expected minimum  
 646 makespan of the rest of the job. Similarly, when the job fails before  
 647 step  $i$ , then that portion is "lost work", and can be denoted by  
 648  $E[L(t, i + \delta)]$  which denotes the expected lost work when there is a  
 649 failure during the time interval  $t$  to  $t + i + \delta$ . A failure before the  
 650 checkpoint means that we have made no progress, and  $W$  steps of  
 651 the job still remain. The expected makespan in the failure case is  
 652 then given by:

$$E[M_{\text{fail}}(W, t, i)] = E[L(t, i + \delta)] + E[M^*(W, t + i + \delta)] \quad (9)$$

653 In the case of memoryless distribution,  $E[L(t, i + \delta)]$  is approxi-  
 654 mated as  $\frac{i+\delta}{2}$ . In our case, we use the failure CDF instead:

$$E[L(t, i + \delta)] = \int_t^{t+i+\delta} xf(x) dx, \quad (10)$$

655 where  $f(x)$  is our probability density function represented by Equa-  
 656 tion 2.

657 Thus we can find the minimum makespan  $E[M^*(W, t)]$  by using  
 658 Equations 6–10. Given a job of length  $J$ , minimizing the total ex-  
 659 pected makespan involves computing  $E[M^*(J, s)]$ , where  $s$  is the  
 660 current age of the server. Since the makespan is recursively defined,  
 661 we can do this minimization using a dynamic programming ap-  
 662 proach, and extract the job-steps at which checkpointing results in  
 663 a minimum expected makespan.

## 5 IMPLEMENTING A BATCH COMPUTING SERVICE FOR PREEMPTIBLE VMs

680 We have implemented an experimental software framework for  
 681 allowing us to implement the various policies for constrained pre-  
 682 emptions. Our goal is to use this service to examine the effectiveness  
 683 of the policies on preemptible VMs under real world conditions.

684 Our service is implemented as a light-weight, extensible frame-  
 685 work that makes it convenient and cheap to run scientific comput-  
 686 ing applications in the cloud. We have implemented our prototype  
 687 in Python in about 2,000 lines of code, and currently support run-  
 688 ning VMs on the Google Cloud Platform [6].

689 Our service is implemented as a centralized controller, which  
 690 implements the VM selection and job scheduling policies described  
 691 in Section ???. The controller can run on any machine (including the  
 692 user's local machine, or inside a cloud VM), and exposes an HTTP  
 693 API to end-users. Users submit bags of jobs to the controller via the  
 694 HTTP API, which then launches and maintains a cluster of cloud  
 695

VMs, and maintains the job queue and metadata in a local database. To improve usability, we automatically generate parameter combinations for a given bag size, based on a user-provided json file with ranges and constraints for each parameter.

Our service integrates, and interfaces with two primary services. First, it uses the Google cloud API [5] for launching, terminating, and monitoring VMs. Once a cluster is launched, it then configures a cluster manager such as Slurm [9] or Torque [11], to which it submits jobs. Our service uses the Slurm cluster manager, with each VM acting as a Slurm “cloud” node, which allows Slurm to gracefully handle VM preemptions. The Slurm master node runs on a small, 2 CPU non-preemptible VM, which is shared by all applications and users. Our service monitors job completions and failures (due to VM preemptions) through the use of Slurm call-backs, which issue HTTP requests back to the service controller.

Our service creates and manages clusters of transient cloud servers, manages all aspects of the VM lifecycle and costs, and implements the various policies described in the rest of this section.

Additionally, our service also incorporates additional functionality to implement a “bag” of jobs that allows multiple jobs to be sequentially run. We observe that many batch jobs, especially scientific simulation workloads, do parameter sweeps.

Specifically, it runs a bag of jobs defined by these parameters:

Bag of job =  $\{\mathcal{A}: \text{Application to execute}, n: \text{Number of jobs}, m: \text{Minimum number of jobs to finish}, \pi: \text{Generator function for job parameters}, \mathcal{R}: \text{Computing resources per job}\}$

We aim to provide a simple user interface to allow users to deploy their applications with minimum workflow changes.

Our service seeks to minimize the cost and running time of bags of jobs of scientific computing applications. Our service’s cost and time minimizing policies for running bags of jobs are based on empirical and analytical models of the cost and preemption dynamics of transient cloud servers, which we present in the next section.

**High-level workflow:** When a user wishes to run a bag of jobs, Our service handles the provisioning of a cluster of transient cloud servers. In addition, Our service deals with the scheduling and monitoring of the bag of jobs, and with VM preemptions.

Our service is designed as a framework that increases the usability and viability of transient cloud servers for scientific computing applications, and Most scientific computing applications are deployed on HPC clusters that have a batch scheduler such as Slurm [9] or Torque [11], and Our service integrates with these schedulers (e.g., Slurm) to provide the same interface to applications. As shown in Figure 4,

## 6 TESTING AND EVALUATION OF MODEL-INFORMED POLICIES

In this section, we present empirical and analytical evaluation of the performance and cost of Our service with different scientific computing workloads and scales. Our evaluation consists of empirical analysis, as well as model-driven simulations for analyzing and comparing Our service behavior under different preemption and application dynamics.

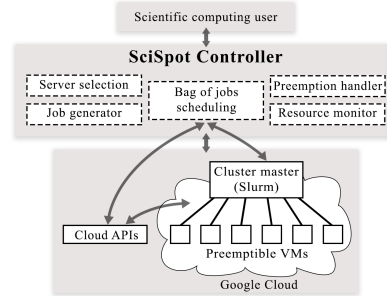


Figure 4: Architecture and system components of our batch computing service.

We shed insight into the fundamental tradeoffs in constrained preemptions, the effectiveness of our model-based policies, and detailed empirical analysis of the cost and performance of our Our service framework with real-world scientific computing applications. We have already established the goodness of fit of our model and compared it to existing models earlier in Section ??.

**Environment and Workloads:** All our empirical evaluation is conducted on the Google Public Cloud, and with these representative scientific computing applications:

**Nanoconfinement.** The nanoconfinement application launches molecular dynamics (MD) simulations of ions in nanoscale confinement created by material surfaces [38, 44].

**Shapes.** The Shapes application runs an MD-based optimization dynamics to predict the optimal shape of deformable, charged nanoparticles [37, 41].

**LULESH.** Livermore Unstructured Lagrangian Explicit Shock Hydrodynamics (LULESH) is a popular benchmark for hydrodynamics simulations of continuum material models [45, 46].

These examples are representative of typical scientific computing applications in the broad domain of physics, materials science, and chemical engineering. These three examples are implemented as parallel programs that use OpenMP and MPI parallel computing techniques. The first two are used in nanoscale materials research [35–38, 41, 64] and LULESH is a widely used benchmark [45, 46]. All applications are run with default parameters unless otherwise stated.

All applications use OpenMPI v2.1.1, are deployed on Slurm v0.4.3 and 64-bit Ubuntu 18.04, and run on Google Cloud VMs with x86-64 Intel Haswell CPUs. For completeness and to guard against concerns about poor cloud performance relative to HPC clusters [18, 30, 34, 52, 79], we benchmarked the Nanoconfinement application on the Big Red II cluster [4]. When run on 4 nodes with 16 CPUs each, the application takes 1140 seconds on Big Red II vs 850 seconds on Our service. We attribute the 20% improvement with Our service to the newer CPUs on Google Cloud (Intel Haswell vs. older 2012-era AMD Opterons in Big Red II).

### 6.1 Tradeoffs In Constrained Preemptions

Below, we analyze the effect of the bathtub shaped preemption curve on application running time.

Preemptions cause jobs to be restarted, which is the *wasted* time, which increases the total running time (i.e, makespan). In the case of constrained preemptions, we evaluate two preemption probability,

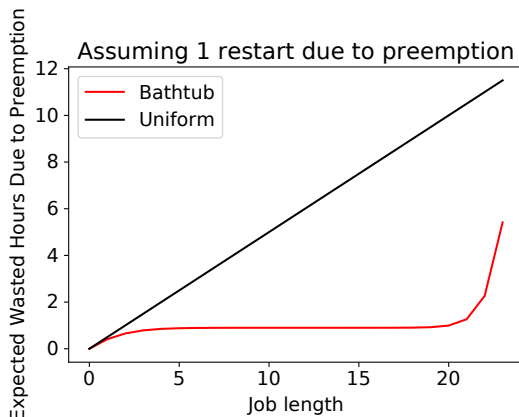


Figure 5: The expected wasted computation, given a single failure, is lower when preemptions are distributed in a bathtub shape, compared to uniformly distributed over the 24 hour interval

the empirically observed bathtub shaped and a uniform distribution of failures.

In Figure 5 we show the expected wasted time *assuming the job suffers a single failure*. We see that in the case of uniform distribution, the increase is linear in the job length. Whereas with bathtub shaped distributions, the mirrors the shape of the CDF, and is constant for all but the largest of jobs.

The expected wasted time is also influenced by the probability of failure, and Figure 6 shows the expected waste. Because preemption rate is high in the initial stages for bathtub failures, for short jobs, the expected waste is higher, because they do not run long enough to take advantage of the low rate of preemptions in the middle stages. If preemptions were uniformly distributed, the waste is quadratic, and given by  $\frac{T^2}{48}$ , and is smaller for short jobs. We see that the “cross over” point is around 5 hours—and for longer jobs, a bathtub preemption behavior is preferable.

(Prateek: Do we give the equations here, or earlier?)

**Result:** For constrained preemptions, bathtub distributions significantly reduce the expected increase in running times for medium to long running jobs, but are slightly inferior for short jobs.

## 6.2 Model-based Policies

We now evaluate our model-driven policies.

**6.2.1 Scheduling.** Our job scheduling policy is model-driven and decides whether to request a new VM for a job or run on an existing VM.

Figure 7 shows the effect of this policy for a job of length 4 hours. We compare against a baseline of existing scheduling policies used by other systems such as ExoSphere . In the absence of insights about bathtub preemptions, the existing frameworks would continue to run on existing server. As the figure shows, for larger jobs the job failure probability is high.

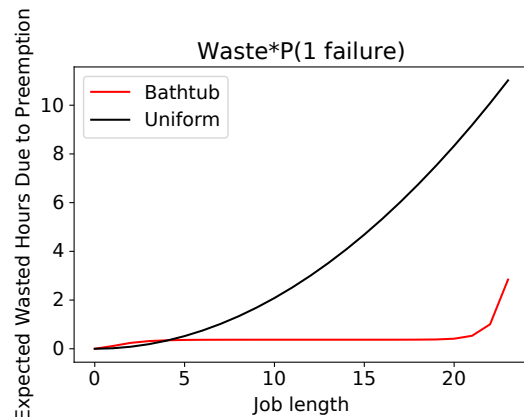


Figure 6: The expected wasted computation is lower when preemptions are distributed in a bathtub shape, compared to uniformly distributed over the 24 hour interval

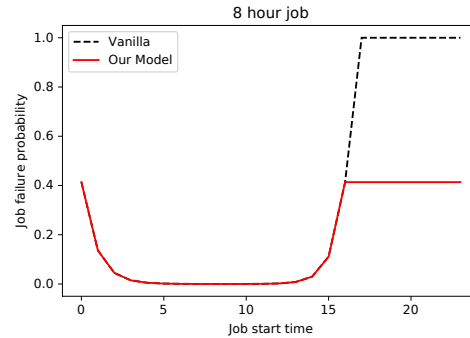


Figure 7: Job failure probability is reduced with the help of our deadline aware scheduling policy, especially for jobs starting near the end of the VM’s lifetime

Figure 8 shows the job failure probability for jobs of different sizes for our model based policy vs a existing vanilla “null” policies that are not informed by the preemption dynamics.

### 6.2.2 Checkpointing.

## 6.3 Evaluation using Typical User-End Scientific Computing Applications

We show the empirical cost and performance and effectiveness of our Our service framework which incorporates our model-based insights and is an easy to use integrated Framework for scientific computing applications.

**6.3.1 Cost.** The primary motivation for using preemptible VMs is their significantly lower cost compared to conventional “on-demand” cloud VMs that are non-preemptible. Figure 12 compares the cost of running different applications with different cloud VM deployments. Our service, which uses both cost-minimizing server selection, and preemptible VMs, results in significantly lower costs

813  
814  
815  
816  
817  
818  
819  
820  
821  
822  
823  
824  
825  
826  
827  
828  
829  
830  
831  
832  
833  
834  
835  
836  
837  
838  
839  
840  
841  
842  
843  
844  
845  
846  
847  
848  
849  
850  
851  
852  
853  
854  
855  
856  
857  
858  
859  
860  
861  
862  
863  
864  
865  
866  
867  
868  
869  
870  
871  
872  
873  
874  
875  
876  
877  
878  
879  
880  
881  
882  
883  
884  
885  
886  
887  
888  
889  
890  
891  
892  
893  
894  
895  
896  
897  
898  
899  
900  
901  
902  
903  
904  
905  
906  
907  
908  
909  
910  
911  
912  
913  
914  
915  
916  
917  
918  
919  
920  
921  
922  
923  
924  
925  
926  
927  
928

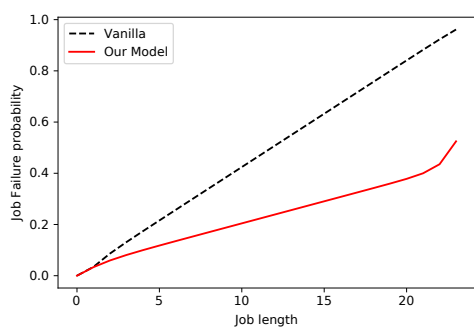


Figure 8: Job failure probability is lower with our deadline aware policy across all job sizes



Figure 9: Checkpointing overhead for jobs of length 4 at different starting times.

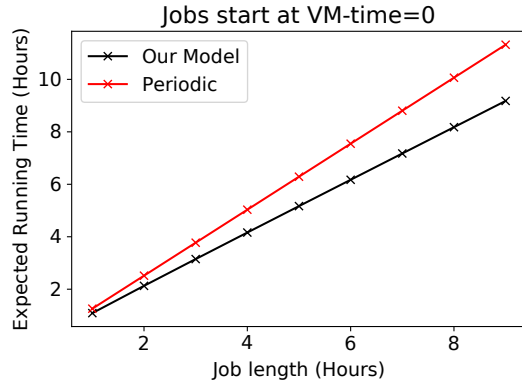


Figure 10: Running time with checkpointing when jobs start at time=0

across the board, even when accounting for preemptions and recomputations. We also compare against ExoSphere [61], a state of the art system for transient server selection. ExoSphere implements

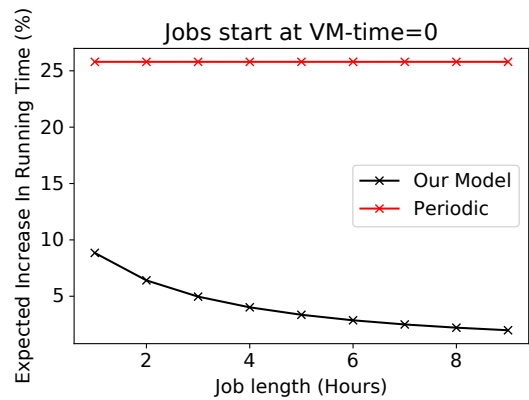


Figure 11: Increase in running time with Checkpointing when jobs start at time =0 (Should be an inset)

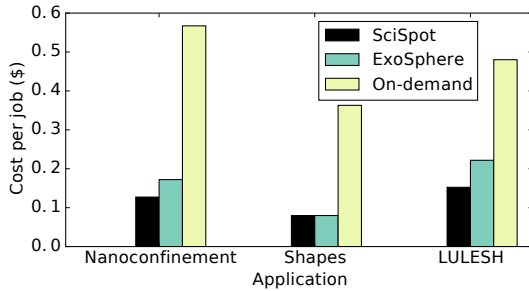


Figure 12: SciSpot’s use of preemptible VMs can reduce costs by up to 5x compared to conventional cloud deployments, and 20% compared to the state of the art EC2 spot instance selection (ExoSphere [61]).

a portfolio-theory approach using EC2 spot prices to balance average cost saving and risk of revocations using diversification and selecting VMs with low price correlation. However, this approach is ineffective for the flat prices of Google Preemptible VMs. Unlike Our service, ExoSphere does *not* consider application performance when selecting servers, and thus is unable to select the best server for parallel applications. Since the Google highcpu VMs have the same price per CPU, ExoSphere picks an arbitrary “median” VM to break ties, which may not necessarily yield the lowest running times. This results in 20% cost increase over Our service.

**Result:** SciSpot reduces computing costs by up to 5x compared to conventional on-demand cloud deployments.

## 7 RELATED WORK

### 7.1 Transient Cloud Computing

The challenges posed by Amazon EC2 spot instances, the first transient cloud servers, have received significant attention from both academia and industry [10]. The significantly lower cost of spot instances makes them attractive for running preemption and delay tolerant batch jobs [21, 27, 39, 48, 66, 73, 77]. The distinguishing characteristic of EC2 spot instances is their dynamic auction-based pricing, and choosing the “right” bid price to minimize cost and performance degradation is the focus of much of the past work on

929  
930  
931  
932  
933  
934  
935  
936  
937  
938  
939  
940  
941  
942  
943  
944  
945  
946  
947  
948  
949  
950  
951  
952  
953  
954  
955  
956  
957  
958  
959  
960  
961  
962  
963  
964  
965  
966  
967  
968  
969  
970  
971  
972  
973  
974  
975  
976  
977  
978  
979  
980  
981  
982  
983  
984  
985  
986  
987  
988  
989  
990  
991  
992  
993  
994  
995  
996  
997  
998  
999  
1000  
1001  
1002  
1003  
1004  
1005  
1006  
1007  
1008  
1009  
1010  
1011  
1012  
1013  
1014  
1015  
1016  
1017  
1018  
1019  
1020  
1021  
1022  
1023  
1024  
1025  
1026  
1027  
1028  
1029  
1030  
1031  
1032  
1033  
1034  
1035  
1036  
1037  
1038  
1039  
1040  
1041  
1042  
1043  
1044

transient computing [33, 40, 53, 65, 68, 72, 74, 75, 78, 80, 81]. However, as explained in Section ??, it remains to be seen how Amazon’s recent change [13] in the preemption model of spot instances affects prior work.

On the other hand, the effective use of transient resources provided by other cloud providers such as Google, Microsoft, Packet, and Alibaba largely remains unexplored. Ours is the first work that studies the preemption characteristics and addresses the challenges involved in running large-scale applications on the Google Preemptible VMs, and provides insights on the unique preemption dynamics.

**7.1.1 Preemption Mitigation.** Effective use of transient servers usually entails the use of fault-tolerance techniques such as checkpointing [60], migration [62], and replication. In the context of HPC workloads, [32, 51, 67] develop checkpointing and bidding strategies for MPI applications running on EC2 spot instances, based on older spot pricing models.

Periodic checkpointing [26] is not optimal in our case because preemptions are not memoryless. By treating bags of jobs as an execution unit, allowing some jobs to fail, and using insights from preemption models, we show that it is possible to reduce the re-computation times to acceptable levels even without the use of periodic checkpointing that imposes additional deployment and performance overheads. Our preemption model for Google preemptible VMs developed in Section 3 provides a novel characterization of bathtub shaped failure rates not captured by the classic Weibull distribution, and is distinct from prior efforts [24, 54].

**7.1.2 Server Selection.** Optimized server selection is an important problem in cloud computing, and especially for transient servers because of the cost-performance-preemption tradeoff involved. Similar to Our service, SpotOn [66] is also a batch computing service that selects servers based on job characteristics and failure rates of different EC2 spot VMs. However, it is restricted to individual, single-VM batch jobs, and its design is tied to EC2 spot instances. The state of the art transient server selection involves the use of multiple types of VMs [61], and selecting a heterogeneous cluster can reduce the likelihood of mass concurrent preemptions. However, since scientific computing applications are mostly synchronous, even a single failure affects the entire job, and heterogeneous clusters are not required, and are in fact, detrimental [61]. Server selection is important even outside of preemptible VMs—developing bayesian optimization and application performance model based search for the “best” cloud VM is an active research area [14, 76], but these techniques do not account for preemptions, which can substantially change the running time characteristics. Investigating these sophisticated search techniques for reducing exploration times is part of our future work.

## 8 CONCLUSION

Given the rise of transient cloud computing and its use in web services and distributed data processing, it is not the question of if, but when, transient cloud computing becomes a credible and powerful alternative to HPC clusters for scientific computing applications. In this paper, we developed principled approaches for deploying and orchestrating scientific computing applications on the cloud, and presented Our service, a framework for low-cost scientific computing on transient cloud servers. Our service develops

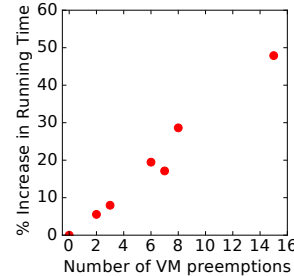


**Figure 13: The increase in running time due to preemptions is under 50%, even at high preemption rates.**

the first empirical and analytical preemption model of Google Preemptible VMs, and uses the model for mitigating preemptions for “bags of jobs”. Our service’s cost-minimizing server selection and job scheduling policies can reduce costs by up to 5× compared to conventional cloud deployments. When compared to HPC clusters, Our service can reduce the total job turnaround times by up to 10×.

## REFERENCES

- [1] Alibaba Cloud Preemptible Instances. <https://www.alibabacloud.com/help/doc-detail/52088.htm>.
- [2] Amazon EC2 Spot Instances, howpublished=<https://aws.amazon.com/ec2/spot/>.
- [3] Azure Low-priority Batch VMs. <https://docs.microsoft.com/en-us/azure/batch/batch-low-pri-vms>.
- [4] Big Red II at Indiana University. <https://kb.iu.edu/d/bcqz>.
- [5] Google Cloud API Documentation. <https://cloud.google.com/apis/docs/overview>.
- [6] Google Cloud Platform. <https://cloud.google.com/>.
- [7] Google Cloud Preemptible VM Instances Documentation, howpublished=<https://cloud.google.com/compute/docs/instances/preemptible>.
- [8] Packet Spot Market. <https://support.packet.com/kb/articles/spot-market>.
- [9] Slurm Workload Manager. <https://slurm.schedmd.com/documentation.html>.
- [10] Spotinst. <https://spotinst.com/>.
- [11] Torque Resource Manager. <http://www.adaptivecomputing.com/products/torque/>.
- [12] Scientific Computing Using Spot Instances. <http://aws.amazon.com/ec2/spot-and-science/>, June 2013.
- [13] New Amazon EC2 Spot pricing model. <https://aws.amazon.com/blogs/compute/new-amazon-ec2-spot-pricing/>, March 2018.
- [14] ALIPOURFARD, O., AND YU, M. CherryPick: Adaptively Unearthing the Best Cloud Configurations for Big Data Analytics. 15.
- [15] AMVROSIADIS, G., PARK, J. W., GANGER, G. R., GIBSON, G. A., BASEMAN, E., AND DEBARDELEBEN, N. On the diversity of cluster workloads and its impact on research results. In *2018 {USENIX} Annual Technical Conference ({USENIX} {ATC} 18)* (2018), pp. 533–546.
- [16] BARTÓK, A. P., DE, S., POELKING, C., BERNSTEIN, N., KERMODE, J. R., CSÁNYI, G., AND CERIOTTI, M. Machine learning unifies the modeling of materials and molecules. *Science Advances* 3, 12 (2017).
- [17] BEN-YEHUDA, O., BEN-YEHUDA, M., SCHUSTER, A., AND TSAFRIR, D. Deconstructing Amazon EC2 Spot Instance Pricing. *ACM TEC* 1, 3 (September 2013).
- [18] BENEDICTIS, A. D., RAK, M., TURTUR, M., AND VILLANO, U. Cloud-Aware Development of Scientific Applications. In *2014 IEEE 23rd International WETICE Conference* (Parma, Italy, June 2014), IEEE, pp. 149–154.
- [19] BOUGERET, M., CASANOVA, H., RABIE, M., ROBERT, Y., AND VIVIEN, F. Checkpointing strategies for parallel jobs. In *Proceedings of 2011 International Conference for High Performance Computing, Networking, Storage and Analysis on - SC ’11* (Seattle, Washington, 2011), ACM Press, p. 1.
- [20] CH’NG, K., CARRASQUILLA, J., MELKO, R. G., AND KHATAMI, E. Machine learning phases of strongly correlated fermions. *Phys. Rev. X* 7 (Aug 2017), 031038.
- [21] CHOCHAN, N., CASTILLO, C., SPREITZER, M., STEINDER, M., TANTAWI, A., AND KRINTZ, C. See Spot Run: Using Spot Instances for MapReduce Workflows. In *HotCloud* (June 2010).
- [22] CIRNE, W., BRASILEIRO, F., SAUVE, J., ANDRADE, N., PARANHOS, D., SANTOS-NETO, E., AND MEDEIROS, R. Grid computing for bag of tasks applications. In *In Proc. of the 3rd IFIP Conference on E-Commerce, E-Business and EGovernment* (2003), IFIP.
- [23] CORTEZ, E., BONDE, A., MUZIO, A., RUSSINOVICH, M., FONTOURA, M., AND BIANCHINI, R. Resource central: Understanding and predicting workloads for improved resource management in large cloud platforms. In *Proceedings of the 26th Symposium on Operating Systems Principles* (New York, NY, USA, 2017), SOSP ’17, ACM, pp. 153–167.
- [24] CREVECOEUR, G. A model for the integrity assessment of ageing repairable systems. *IEEE Transactions on reliability* 42, 1 (1993), 148–155.

- 1161 [25] DALY, J. T. A Higher Order Estimate of the Optimum Checkpoint Interval for  
1162 Restart Dumps. *Future Generation Computer Systems* 22, 3 (2006).
- 1163 [26] DONGARRA, J., HERAULT, T., AND ROBERT, Y. Fault tolerance techniques for  
1164 high-performance computing. 66.
- 1165 [27] DUBOIS, D. J., AND CASALE, G. Optispot: minimizing application deployment cost  
1166 using spot cloud resources. *Cluster Computing* (2016), 1–17.
- 1167 [28] FERGUSON, A. L. Machine learning and data science in soft materials engineering.  
*Journal of Physics: Condensed Matter* 30, 4 (2017), 043002.
- 1168 [29] FOX, G., GLAZIER, J. A., KADUPUTTYA, J., JADHAO, V., KIM, M., QIU, J., SLUKA, J. P.,  
1169 SOMOGYI, E., MARATHE, M., ADIGA, A., ET AL. Learning Everywhere: Pervasive  
1170 machine learning for effective High-Performance computation. *arXiv preprint arXiv:1902.10810* (2019).
- 1171 [30] GALANTE, G., ERPEN DE BONA, L. C., MURY, A. R., SCHULZE, B., AND DA ROSA RIGHI,  
1172 R. An Analysis of Public Clouds Elasticity in the Execution of Scientific Applications:  
1173 a Survey. *Journal of Grid Computing* 14, 2 (June 2016), 193–216.
- 1174 [31] GARÃN, Y., MONGE, D. A., MATEOS, C., AND GARCÃN GARINO, C. Learning  
1175 budget assignment policies for autoscaling scientific workflows in the cloud.  
*Cluster Computing* (Feb. 2019).
- 1176 [32] GONG, Y., HÈ, B., AND ZHOU, A. C. Monetary cost optimizations for MPI-based  
1177 HPC applications on Amazon clouds: checkpoints and replicated execution. In  
1178 *Proceedings of the International Conference for High Performance Computing,  
Networking, Storage and Analysis on - SC '15* (Austin, Texas, 2015), ACM Press,  
pp. 1–12.
- 1179 [33] GUO, W., CHEN, K., WU, Y., AND ZHENG, W. Bidding for Highly Available Services  
1180 with Low Price in Spot Instance Market. In *Proceedings of the 24th International  
Symposium on High-Performance Parallel and Distributed Computing - HPDC '15*  
(Portland, Oregon, USA, 2015), ACM Press, pp. 191–202.
- 1181 [34] IOSUP, A., OSTERMANN, S., YIGITBASI, M. N., PRODAN, R., FAHRINGER, T., AND  
1182 EPEMA, D. H. J. Performance Analysis of Cloud Computing Services for Many-  
1183 Tasks Scientific Computing. *IEEE Transactions on Parallel and Distributed Systems*  
22, 6 (June 2011), 931–945.
- 1184 [35] JADHAO, V., SOLIS, F. J., AND OLVERA DE LA CRUZ, M. Simulation of charged  
1185 systems in heterogeneous dielectric media via a true energy functional. *Phys. Rev. Lett.* 109 (Nov 2012), 223905.
- 1186 [36] JADHAO, V., SOLIS, F. J., AND OLVERA DE LA CRUZ, M. A variational formulation  
1187 of electrostatics in a medium with spatially varying dielectric permittivity. *The Journal of  
Chemical Physics* 138, 5 (2013), 054119.
- 1188 [37] JADHAO, V., THOMAS, C. K., AND OLVERA DE LA CRUZ, M. Electrostatics-driven  
1189 shape transitions in soft shells. *Proceedings of the National Academy of Sciences*  
111, 35 (2014), 12673–12678.
- 1190 [38] JADHAO, V., YAO, Z., THOMAS, C. K., AND DE LA CRUZ, M. O. Coulomb energy  
1191 of uniformly charged spheroidal shell systems. *Physical Review E* 91, 3 (2015),  
032305.
- 1192 [39] JAIN, N., MENACHE, I., AND SHAMIR, O. On-demand, spot, or both: Dynamic  
1193 resource allocation for executing batch jobs in the cloud. In *11th International  
Conference on Autonomic Computing (ICAC 14)*, USENIX Association.
- 1194 [40] JAVADI, B., THULASIRAM, R., AND BUYYA, R. Statistical Modeling of Spot Instance  
1195 Prices in Public Cloud Environments. In *UCC* (December 2011).
- 1196 [41] JING, Y., JADHAO, V., ZWANIKKEN, J. W., AND OLVERA DE LA CRUZ, M. Ionic  
1197 structure in liquids confined by dielectric interfaces. *The journal of chemical  
physics* 143, 19 (2015), 194508.
- 1198 [42] JOAQUIM, P., BRAVO, M., RODRIGUES, L., AND MATOS, M. Hourglass: Leveraging  
1199 transient resources for time-constrained graph processing in the cloud. In *Proceedings  
of the Fourteenth EuroSys Conference 2019* (New York, NY, USA, 2019),  
EuroSys '19, ACM, pp. 35:1–35:16.
- 1200 [43] KADUPUTTYA, J., FOX, G., AND JADHAO, V. Machine Learning for Performance  
1201 Enhancement of Molecular Dynamics Simulations. In *Proceedings of the International  
Conference on Computational Science (ICCS) 2019* (2019), Springer.
- 1202 [44] KADUPUTTYA, J., MARRU, S., FOX, G. C., AND JADHAO, V. Ions in nanocon-  
1203 finement, Dec 2017. Online on nanoHUB; source code on GitHub at  
1204 [github.com/softmaterialslab/nanoconfinement-md](https://github.com/softmaterialslab/nanoconfinement-md).
- 1205 [45] KARLIN, I., BHATELE, A., KEASLER, J., CHAMBERLAIN, B. L., COHEN, J., DEVITO, Z.,  
1206 HAQUE, R., LANAY, D., LUKE, E., WANG, F., RICHARDS, D., SCHULZ, M., AND STILL,  
1207 C. Exploring traditional and emerging parallel programming models using a  
1208 proxy application. In *27th IEEE International Parallel & Distributed Processing  
Symposium (IEEE IPDPS 2013)* (Boston, USA, May 2013).
- 1209 [46] KARLIN, I., KEASLER, J., AND NEELY, R. Lulesh 2.0 updates and changes. Tech. Rep.  
1210 LLNL-TR-641973, August 2013.
- 1211 [47] KLIMECK, G., McLENNAN, M., LUNDSTROM, M. S., AND ADAMS III, G. B. nanohub.  
org-online simulation and more materials for semiconductors and nanoelectronics  
1212 in education and research, 2008.
- 1213 [48] LIU, H. Cutting MapReduce Cost with Spot Market. In *HotCloud* (June 2011).
- 1214 [49] LIU, J., QI, Y., MENG, Z. Y., AND FU, L. Self-learning monte carlo method. *Phys.  
Rev. B* 95 (Jan 2017), 041101.
- 1215 [50] LONG, A. W., ZHANG, J., GRANICK, S., AND FERGUSON, A. L. Machine learning  
1216 assembly landscapes from particle tracking data. *Soft Matter* 11, 41 (2015), 8141–  
8153.
- 1217 [51] MARATHE, A., HARRIS, R., LOWENTHAL, D., DE SUPINSKI, B. R., ROUNTREE, B., AND  
1218 SCHULZ, M. Exploiting redundancy for cost-effective, time-constrained execution  
1219 of hpc applications on amazon ec2. In *HPDC* (2014), ACM.
- 1220 [52] MARATHE, A., HARRIS, R., LOWENTHAL, D. K., DE SUPINSKI, B. R., ROUNTREE,  
1221 B., SCHULZ, M., AND YUAN, X. A comparative study of high-performance computing  
1222 on the cloud. In *Proceedings of the 22nd international symposium on High-performance  
parallel and distributed computing* (2013), ACM, pp. 239–250.
- 1223 [53] MIHAILESCU, M., AND TEO, Y. M. The Impact of User Rationality in Federated  
1224 Clouds. In *CCGrid* (2012).
- 1225 [54] MUDHOLKAR, G. S., AND SRIVASTAVA, D. K. Exponentiated weibull family for  
1226 analyzing bathtub failure-rate data. *IEEE transactions on reliability* 42, 2 (1993),  
299–302.
- 1227 [55] NETTO, M. A. S., CALHEIROS, R. N., RODRIGUES, E. R., CUNHA, R. L. F., AND BUYYA,  
1228 R. Hpc cloud for scientific and business applications: Taxonomy, vision, and  
1229 research challenges. *ACM Comput. Surv.* 51, 1 (Jan. 2018), 8:1–8:29.
- 1230 [56] OPRESCU, A., AND KIELMANN, T. Bag-of-tasks scheduling under budget constraints.  
In *2010 IEEE Second International Conference on Cloud Computing Technology and  
Science* (Nov 2010), pp. 351–359.
- 1231 [57] OUYANG, X., IRWIN, D., AND SHENOY, P. Spotlight: An information service for  
1232 the cloud. In *IEEE International Conference on Distributed Computing Systems  
(ICDCS) 2016*.
- 1233 [58] SCHOENHOLZ, S. S. Combining machine learning and physics to understand glassy  
1234 systems. *Journal of Physics: Conference Series* 1036, 1 (2018), 012021.
- 1235 [59] SHARMA, P. Transiency-driven Resource Management for Cloud Computing  
1236 Platforms. [https://scholarworks.umass.edu/dissertations\\_2/1388/](https://scholarworks.umass.edu/dissertations_2/1388/), 2018.
- 1237 [60] SHARMA, P., GUO, T., HE, X., IRWIN, D., AND SHENOY, P. Flint: Batch-Interactive  
1238 Data-Intensive Processing on Transient Servers. In *EuroSys* (April 2016).
- 1239 [61] SHARMA, P., IRWIN, D., AND SHENOY, P. Portfolio-driven resource management  
1240 for transient cloud servers. In *Proceedings of ACM Measurement and Analysis of  
Computer Systems* (June 2017), vol. 1, p. 23.
- 1241 [62] SHARMA, P., LEE, S., GUO, T., IRWIN, D., AND SHENOY, P. SpotCheck: Designing a  
1242 Derivative IaaS Cloud on the Spot Market. In *EuroSys* (April 2015).
- 1243 [63] SILBERSTEIN, M., SHAROV, A., GEIGER, D., AND SCHUSTER, A. Gridbot: execution  
1244 of bags of tasks in multiple grids. In *Proceedings of the Conference on High  
Performance Computing Networking, Storage and Analysis* (Nov 2009), pp. 1–12.
- 1245 [64] SOLIS, F. J., JADHAO, V., AND DE LA CRUZ, M. O. Generating true minima in  
1246 constrained variational formulations via modified lagrange multipliers. *Physical  
Review E* 88, 5 (2013), 053306.
- 1247 [65] SONG, Y., ZAFER, M., AND LEE, K. Optimal Bidding in Spot Instance Market. In  
1248 *Infocom* (March 2012).
- 1249 [66] SUBRAMANYA, S., GUO, T., SHARMA, P., IRWIN, D., AND SHENOY, P. SpotOn: A  
1250 Batch Computing Service for the Spot Market. In *SOCC* (August 2015).
- 1251 [67] TAIFI, M., SHI, J. Y., AND KHREISHAH, A. SpotMPI: A Framework for Auction-Based  
1252 HPC Computing Using Amazon Spot Instances. In *Algorithms and Architectures  
for Parallel Processing*, Y. Xiang, A. Cuzocrea, M. Hobbs, and W. Zhou, Eds.,  
vol. 7017. Springer Berlin Heidelberg, Berlin, Heidelberg, 2011, pp. 109–120.
- 1253 [68] TANG, S., YUAN, J., AND LI, X. Towards Optimal Bidding Strategy for Amazon  
1254 EC2 Cloud Spot Instance. In *CLOUD* (June 2012).
- 1255 [69] VARSHNEY, P., AND SIMMHAN, Y. AutoBoT: Resilient and Cost-effective Scheduling  
1256 of a Bag of Tasks on Spot VMs. *IEEE Transactions on Parallel and Distributed  
Systems* (2019), 1–1.
- 1257 [70] VERMA, A., PEDROSA, L., KORUPOLU, M., OPPENHEIMER, D., TUNE, E., AND WILKES,  
J. Large-scale cluster management at google with borg. In *EuroSys* (2015), ACM.
- 1258 [71] WARD, L., DUNN, A., FAGHANINIA, A., ZIMMERMANN, N. E., BAJAJ, S., WANG, Q.,  
MONTOYA, J., CHEN, J., BYSTROM, K., DYLLA, M., ET AL. Matminer: An open source  
1259 toolkit for materials data mining. *Computational Materials Science* 152 (2018),  
60–69.
- 1260 [72] WEE, S. Debunking Real-Time Pricing in Cloud Computing. In *CCGrid* (May  
2011).
- 1261 [73] WIEDER, A., BHATOTIA, P., POST, A., AND RODRIGUES, R. Orchestrating the  
1262 deployment of computations in the cloud with conductor. In *NSDI 12* (2012).
- 1263 [74] WOLSKI, R., BREVIK, J., CHARD, R., AND CHARD, K. Probabilistic guarantees of  
1264 execution duration for Amazon spot instances. In *Proceedings of the International  
Conference for High Performance Computing, Networking, Storage and Analysis on  
- SC '17* (Denver, Colorado, 2017), ACM Press, pp. 1–11.
- 1265 [75] XU, H., AND LI, B. A Study of Pricing for Cloud Resources. *Performance Evaluation  
Review* 40, 4 (March 2013).
- 1266 [76] YADWADKAR, N. J., HARIHARAN, B., GONZALEZ, J. E., SMITH, B., AND KATZ, R. H.  
1267 Selecting the best VM across multiple public clouds: a data-driven performance  
modeling approach. In *Proceedings of the 2017 Symposium on Cloud Computing -  
SoCC '17* (Santa Clara, California, 2017), ACM Press, pp. 452–465.
- 1268 [77] YI, S., KONDO, D., AND ANDRZEJK, A. Reducing costs of spot instances via  
1269 checkpointing in the amazon elastic compute cloud. In *Cloud Computing (CLOUD),  
2010 IEEE 3rd International Conference on* (2010), IEEE, pp. 236–243.
- 1270 [78] ZAFER, M., SONG, Y., AND LEE, K. Optimal Bids for Spot VMs in a Cloud for  
1271 Deadline Constrained Jobs. In *CLOUD* (2012).
- 1272

, ,		
1277	[79] Zhai, Y., Liu, M., Zhai, J., Ma, X., and Chen, W. Cloud versus in-house cluster: evaluating Amazon cluster compute instances for running MPI applications. In <i>State of the Practice Reports on - SC '11</i> (Seattle, Washington, 2011), ACM Press, p. 1.	1335
1278		1336
1279	[80] Zhang, Q., Gürses, E., Boutaba, R., and Xiao, J. Dynamic Resource Allocation for Spot Markets in Clouds. In <i>Hot-ICE</i> (March 2011).	1337
1280	[81] Zheng, L., Joe-Wong, C., Tan, C. W., Chiang, M., and Wang, X. How to Bid the Cloud. In <i>SIGCOMM</i> (August 2015).	1338
1281		1339
1282		1340
1283		1341
1284		1342
1285		1343
1286		1344
1287		1345
1288		1346
1289		1347
1290		1348
1291		1349
1292		1350
1293		1351
1294		1352
1295		1353
1296		1354
1297		1355
1298		1356
1299		1357
1300		1358
1301		1359
1302		1360
1303		1361
1304		1362
1305		1363
1306		1364
1307		1365
1308		1366
1309		1367
1310		1368
1311		1369
1312		1370
1313		1371
1314		1372
1315		1373
1316		1374
1317		1375
1318		1376
1319		1377
1320		1378
1321		1379
1322		1380
1323		1381
1324		1382
1325		1383
1326		1384
1327		1385
1328		1386
1329		1387
1330		1388
1331		1389
1332		1390
1333		1391
1334		1392